THE PENNSYLVANIA STATE UNIVERSITY
SCHREYER HONORS COLLEGE

DEPARTMENT OF BIOENGINEERING

MAGNETIC RESONANCE IMAGING AS A DIAGNOSTIC TOOL IN THE DETECTION OF DIABETIC RETINOPATHY IN MICE

KEALAN HOBELMANN
Semester of Graduation: Spring 2012

A thesis
submitted in partial fulfillment
of the requirements
for a baccalaureate degree
in Nuclear Engineering
with honors in Bioengineering

Reviewed and approved* by the following:

Dr. Thomas Neuberger
Assistant Professor of Bioengineering
Thesis Supervisor

Dr. Peter Butler
Associate Professor of Bioengineering
Honors Adviser

* Signatures are on file in the Schreyer Honors College.

ABSTRACT

Diabetic retinopathy (DR) is a diabetes-induced condition which can lead to significant vision loss or complete blindness. As retinal tissues begin to suffer from ischemia, vascular endothelial growth factor (VEGF) is produced to begin the formation of new vessels. In many cases, the new vessels are prone to hemorrhaging leading to conditions such as neovascular glaucoma, vitreous hemorrhaging, detached retina, and macular edema. It is proposed that magnetic resonance imaging can be used to measure retinal perfusion in order to detect the vascular changes which precede the onset of DR. For improved contrast, arterial spin labeling may be used in a gradient echo sequence to observe retinal perfusion while disregarding the signal from eye tissues. Using VEGF to induce neovascularization in mice, it is possible to observe the changes which take place in the retina during the course of DR to later be applied to human diagnostic techniques. This investigation focuses on the construction of the required radiofrequency coil as well as the experimental design.

TABLE OF CONTENTS

LIST OF FIGURES

ACKNOWLEDGEMENTS

First and foremost, I would like to thank my thesis adviser, Dr. Thomas Neuberger, whose guidance and extensive knowledge helped me through every step of the design process. I would also like to thank Dr. Peter Butler for welcoming me into the bioengineering family despite the growing number of bioengineering honors students. I wish luck to Rohit Ananth who has been a friend and support through the design project and will be continuing the research in the future. Finally, I offer my regards and blessings to all of those who supported me in any other respect during the completion of the project.

Kealan Hobelmann

Chapter 1

Introduction

Diabetic retinopathy has been widely accepted as a leading cause of blindness in adults between the ages 25-74 in the United States (Bhavsar, 2011). According to J.G. Cunha-Vaz of the University of Coimbra, the reported blindness registrations which are linked directly to diabetes have increased to over 15 million cases per year in the United States alone and the number is increasing globally each year (Laatikainen, 1976). Both Type I and Type II Diabetes have been shown to cause retinopathy, although the condition is more common for people with Type I.

Pathophysiology

The eye is largely composed of the vitreous humor, a clear gel that fills the space in the center of the eye. Anterior to the eye is the lens, followed by the iris. The outermost encompassing layer of tissue which contains the eye is called the sclera. Inside the sclera is a layer of blood vessels which provide oxygen to several of the structures of the eye including the ciliary body and the iris. Inwards from the choroid layer is the retina which contains photoreceptor cells that transmit photons from incoming light to nervous signals which travel to the brain. The center of the retina in the back of the eye is called the macula. This is the region of the retina which is responsible for the central field of view.

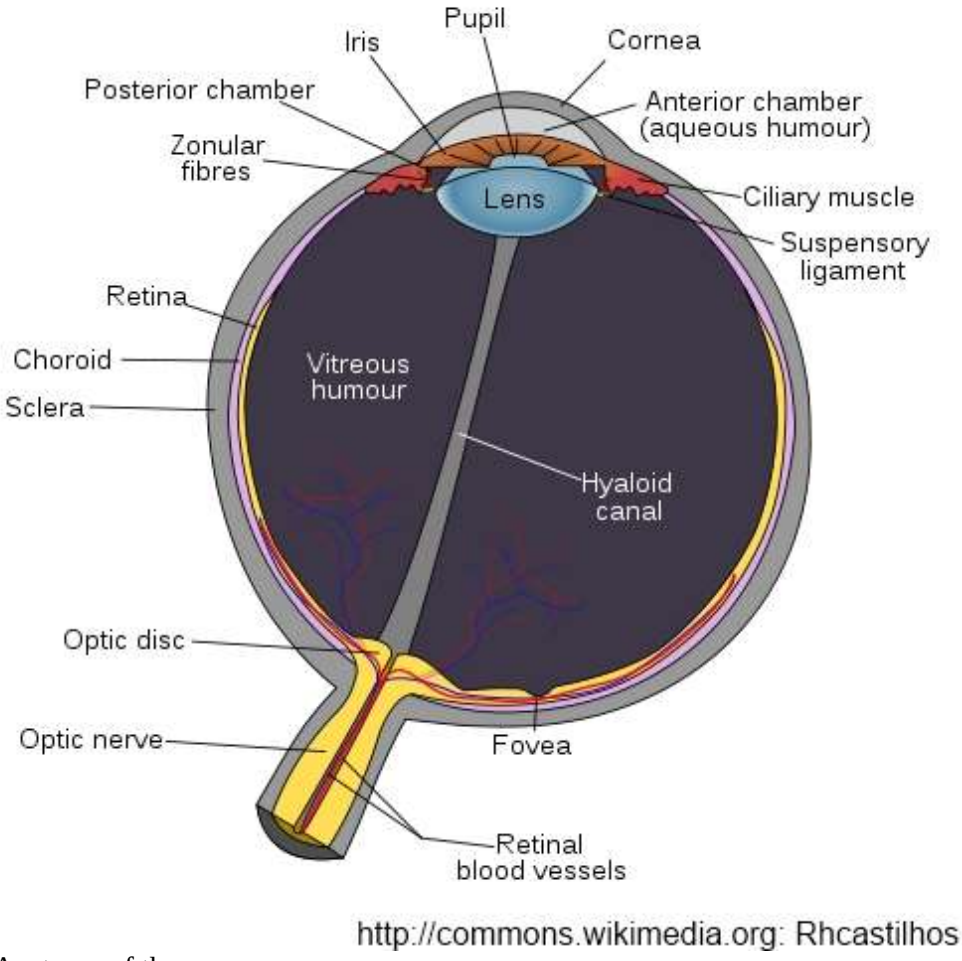

Figure 1: Anatomy of the eye

According to Figure 2, the vascular retinal layer is approximately 80 μm thick and the choroid layer is approximately 42 μm thick. There is a space in between the layers in which no vasculature is present. Because of this space, the blood vessels in each layer are able to be resolved.

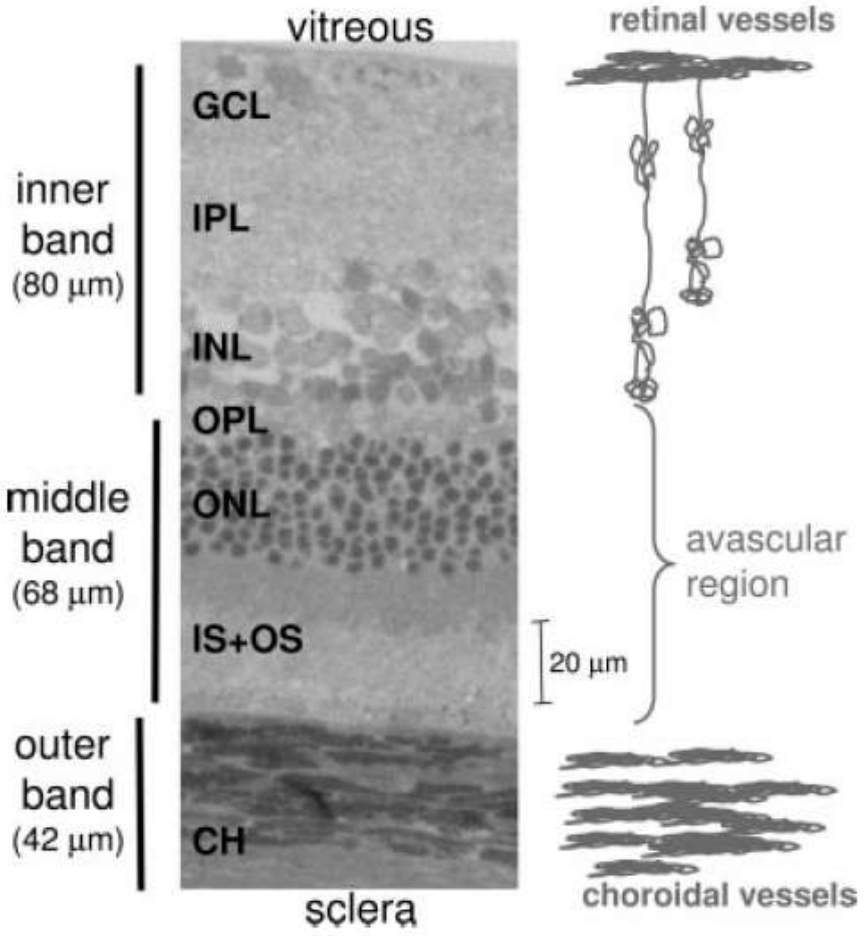

Figure 2: Choroid and retinal layers of the eye. From: Cheng H et al,PNAS 103, 46 17525-17530 (2006)

The earliest signs of retinopathy typically present as microaneurysms on the venous side of small retinal capillaries at the back of the eye. This stage, referred to as "mild nonproliferative retinopathy," generally does not involve any form of vision loss and is therefore difficult to diagnose. As the disease progresses, the arterial side of retinal capillaries may begin to experience epithelial cell death and flow blockage. To compensate, some capillaries become enlarged and serve as an arterial shunt to move blood through the retina. In severe nonproliferative retinopathy, blockages in the

capillaries increase greatly, causing nutrient deprivation in several areas of the retinal tissue. It has been shown that hypoxia caused by lack of perfusion in retinal pigment epithelial cells induces vascular endothelial growth factor (VEGF) to be produced in the retina (Aiello, 1995). VEGF is responsible for the neovascularization of new retinal capillaries, marking the transition to full proliferative retinopathy.

People with proliferative retinopathy are at risk for blindness if not treated immediately. Because the newly formed vasculature is abnormal and fragile relative to the native capillaries, there is a high risk of hemorrhage in the thin walls. While these newly formed vessels remain intact, there may be no obvious signs of vision impairment to the subject. However, because the new vasculature is weak, it is prone to hemorrhage suddenly if placed under stress. This condition, called a vitreous hemorrhage, causes blood to leak from the retinal blood vessels into the vitreous humor. As blood leaks into the vitreous humor, light is inhibited from reaching the photoreceptors at the back of the retina leading to blurred or splotchy vision or in severe cases complete blindness.

Figure 3: Proliferative diabetic retinopathy showing extensive retinal hemorrhages and neovascularization.

In some cases, new vessels may form closer to the front of the eye covering the iris. Vessel formation in this region can cause the Canal of Schlemm to become blocked, inhibiting drainage of the aqueous humor. If left unchecked, the pressure buildup in the aqueous chamber can cause a form of glaucoma called neovascular glaucoma (Laatikainen, 1976).

Hemorrhaging of the retinal blood vessels may also cause the retina to become detached. Once vessels begin to leak, the body responds by forming scar tissue to seal the breaks. Scar tissue, unlike retinal and vitreous tissue, is not pliable and often generates tension between the surfaces it borders. In some cases, stresses created by the scar tissue are sufficient to pull the retina from the outer layers of the eye leading to immediate vision impairment (Laatikainen, 1976).

Finally, the increased permeability of the new vessels can lead to macular edema over time. Fluid builds up in the macula causing it to swell and deform, thereby blurring or distorting the central vision controlled by the macular portion of the retina.

There are treatments for each of these conditions, however by the time the condition is diagnosed the disease is often well-progressed (Berkowitz, 2003). Unfortunately, full vision restoration is not possible for many diabetics suffering from retinopathy.

Current Diagnostic Strategies

Current diagnostic techniques tend to only be effective after neovascularization and hemorrhaging have begun. For this reason, it is difficult to confront the underlying conditions in the early stages. The primary diagnostic measure currently employed for diabetic retinopathy is funduscopic imaging. During this procedure, a doctor or ophthalmologist shines a light onto the retina while looking through a lens. A reflected image of the retina is visible which can be used to observe pathologies of the retina. While funduscopic imaging is useful in confirming damage caused by diabetic retinopathy, it is only useful after irreversible damage is done to the retina causing lasting visual impairment.

Figure 4: Image of an eye using funduscopic imaging.

Another common practice involves a type of angiography using colored fluorescein dye to make the retinal vasculature more visible. Fluorescein specifically targets the retinal blood vessels over other choroidal vessels, making it ideal for use with retinopathy patients. However, according to a study performed by researchers at the Moorfields Eye Hospital in London, the use of fluorescein angiography on patients during their first month of visual symptoms was of prognostic value only for those patients with a poor prognosis. In other words, the procedure is not very useful for patients who do not already present lasting retinal damage (Laatikainen, 1976). While fluorescein angiography is an important tool for identifying proliferative diabetic retinopathy in order to slow its progression, another imaging technique is necessary for earlier detection to allow complete vision preservation in diabetic patients.

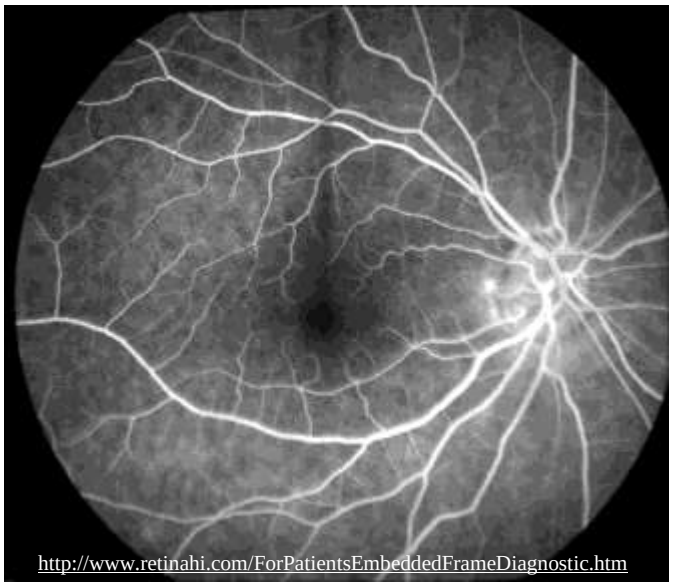

Figure 5: Image taken of an eye using angiography to reconstruct the vascular structure.

A more advanced method involves the use of optical coherence tomography (OCR) to determine changing thickness in the retina. The imaging technique, sometimes described as "optical ultrasound," can produce an image of opaque tissues with a high degree of accuracy. OCR is primarily used to determine changes in retinal thickness. Therefore, the primary prognostic benefit of OCR is in early detection of macular edema, a common symptom of diabetic retinopathy causing fluid accumulation in the macular region of the retina. However, because OCR is dependent on the attenuation of light through the eye, barriers such as vitreous hemorrhages, also common to retinopathy patients, may complicate collection of diagnostically relevant images. More importantly, the discovery of macular edema is only possible after some level of disease progression in retinal tissue, thus limiting the possibility of early detection.

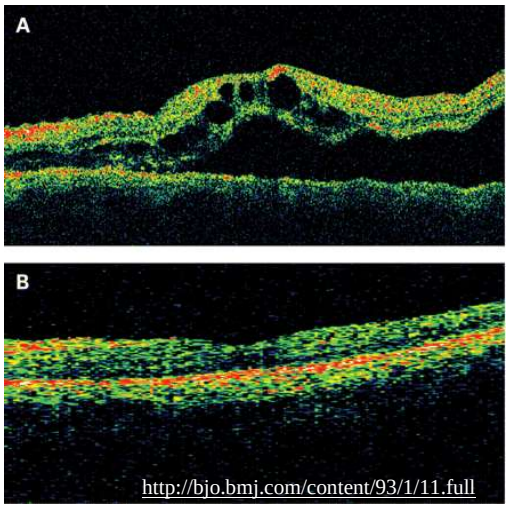

Figure 6: Image of a damaged retina (A) and healthy retina (B) using OCR

Magnetic Resonance Imaging

A major issue with all of the above optical techniques is the lack of depth that can be analyzed. Magnetic resonance imaging (MRI) has the potential to provide early prognoses for diabetic retinopathy based on fully dimensional image measurements of blood flow and oxygen content. While most other methods of detection involve the surface observation of pathological tissue, several studies have shown that dimensional reconstruction using MRI may be able to detect subtle changes to the retinal environment before the onset of the later stages of nonproliferative retinopathy (Berkowitz, 2003)(Trick, 2008). More importantly, all optical techniques are primarily qualitative in nature. MRI introduces the potential for quantitative analysis of blood flow using contrast agents.

The retina is a very metabolically active tissue and therefore requires constant perfusion to supply enough oxygen to the surrounding cells. Blood-oxygen level

dependent functional MRI (BOLD fMRI) involves measuring the oxygenation level of retinal blood supplies in control and diabetic subjects. Diabetic subjects with damaged retinas have more difficulty regulating the level of oxygen perfusion to retinal tissues. Therefore, when exposed to hyperbolic oxygen supplies, diabetic patients show a significant increase in oxygen content in the tissue surrounding the retina. In one study, two groups were exposed to high oxygen levels: a control group and a diabetic group. While both groups showed increased levels of blood oxygen, the control group began to level off after 40 minutes. The diabetic group, however, continued to increase in pO2 (Trick, 2008).

A more common technique involves *in vivo* mapping of retinal blood flows in normal and pathological circumstances. It is already widely accepted that blood flow can be measured quantitatively in the brain using functional MRI (Sicard, 2003). However, relative to optical techniques, MRI yields images with a lower special resolution and signal to noise ratio (Muir, 2010). The retina and choroid layers of rodents have a combined thickness of approximately 250 μm (Cheng, 2006). Therefore, the primary barrier to full diagnostic use of MRI in detecting diabetic retinopathy is the need for finer resolution images.

Evidence has shown that the retinal and choroid layers of the eye could be distinguished using arterial spin labeling (ASL) (Muir, 2010). This technique involves the use of a transmitting and receiving coil which is placed over the region of interest and a labeling coil placed over the heart. By saturating the endogeneous water in the blood leaving the aorta, the eye resonator may be configured to only receive signal from the eye tissues using a gradient echo. During a subsequent scan, no arterial spin labeling is

performed to allow signal from both the eye tissues and the blood to be imaged. By subtracting the signal from the eye tissues from the complete eye image, the signal from blood in retinal and choroid tissues may be isolated (Muir, 2010).

This investigation seeks to expand on this imaging technique by applying vascular endothelial growth factor (VEGF) to an animal subject to induce neovascularization. Using ASL technique, the newly formed blood vessels may be observed. Retinal blood flow rates may also be observed quantitatively for direct comparison to healthy tissue.

Previous Radiofrequency Coil Design

Figure 7: Original RF coil used to hold animal during image scans. A copper shield was placed over the entire open section of the coil.

A previous study was performed on diabetic C57BL/6 mice using a custom built radiofrequency coil to image the vessels on the retina. Figure 7 shows the animal bed of the coil. The design features a side mounted surface coil which is placed directly over the left eye. The coil is somewhat adjustable via the ridged plastic beneath the bed. Not shown is a U-shaped support which sits under the animal's neck. On either end of the U

are two small rods which can be placed into the animal's ears for further support, though the exact placement is difficult.

Much of the effort involved producing images with a high enough resolution to distinguish between the different layers of the retina and choroid in the eyes of mice. From the resolution which was obtainable, no significant differences were found between mice with diabetes and those without.

The purpose of this investigation is to design a custom radiofrequency coil which can incorporate a two coil system for arterial spin labeling. Several limiting factors were identified in the previous coil design, which are also addressed in the new design.

Chapter 2

Objective

The objective of this study is to design a radiofrequency coil which can incorporate a dual coil system for arterial spin labeling. After construction, the coil must be capable of achieving a resolution small enough to distinguish the choroid and retina eye layers in C57BL/6 mice.

Identification of Imaging Problems

Most design considerations were derived from the previous custom built radiofrequency coil used to image retinal blood vessels in C57BL/6 mice. Three primary design objectives were identified in order to increase image resolution and quality.

First, it was determined that increased heat was needed to prevent the blood flow from slowing when the animal is under isoflorane. As the body temperature of the animal increases, the blood vessels dilate making imaging easier and of higher quality. In many cases, the body temperature drops during sleep. Therefore, the design must incorporate a mechanism for heating the animal consistently for the duration of the imaging scan, without interfering with the magnetic field gradient.

Second, increased animal stabilization was necessary. Motion artifacts are a common problem when imaging fine detail samples using NMR. In order to accurately observe the retinal blood vessels, motion during the scans had to be reduced as much as reasonably possible. In particular, test scans revealed a type of "hiccup breathing" which

resulted from low respiratory rates. Motion is impossible to eliminate due to respiration and circulation. However, this must be limited as much as possible, surrounding the head.

Finally, a two-coil system and imaging sequence was identified as a possible way to increase the effectiveness of retinal imaging. Using a technique originated by Eric Muir and Timothy Duong, a labeling coil will be placed over the region of the mouse's heart (Muir, 2010). This coil will be used to excite the protons in the blood leaving the heart in the aorta. A receiving coil will be placed in a similar position to the original RF coil in order to interpret the signal produced by the retinal blood supply. Ideally, by labeling the blood in the heart and receiving the signal from a separate coil, there will be a stronger contrast between vessels and other retinal tissue present in the eye. It is important to ensure that there is no interference between the two coils during the pulse sequence. According to Muir, 2.3 cm is a large enough distance to prevent any interference (Muir, 2010).

Chapter 3

Design

Design Process

The design process consisted of an iterative process of problem identification, design, and prototyping. The three primary design concerns were identified as: maintaining body temperature, limiting motion-induced artifacts, and incorporating two radiofrequency surface coils without interference.

The process began with an analysis of the current coil design in use for retinal imaging in mice. The dimensions of most components were recorded and general design methodology was observed. In addition, general background research was performed.

Some existing materials were gathered which could be reused from past coil designs, most notably the aluminum casing. Both the 1.25” and 2” tubing used for structural components had already been obtained, leading to their incorporation in the final design.

Several iterations of designing and prototyping were performed. Each prototype helped to identify further considerations for the final design. Any materials which had not been acquired were procured from McMaster -Carr.

Structure and Stability

The primary structural component of the radiofrequency coil is the aluminum casing which houses a majority of the components. The casing is 2.15” in outside

diameter allowing for a tight fit in the 14T Varian imaging magnet. On the bottom, an aluminum plate was fixed which holds the BNC connection points when assembled. An end plate was also attached which may be adjusted along the length of the casing using three friction screws. The end plate was set to ensure the coil did not protrude too deeply into the magnet. Finally, 12 filleted holes were drilled sequentially along one side for attachment and placement of inside components.

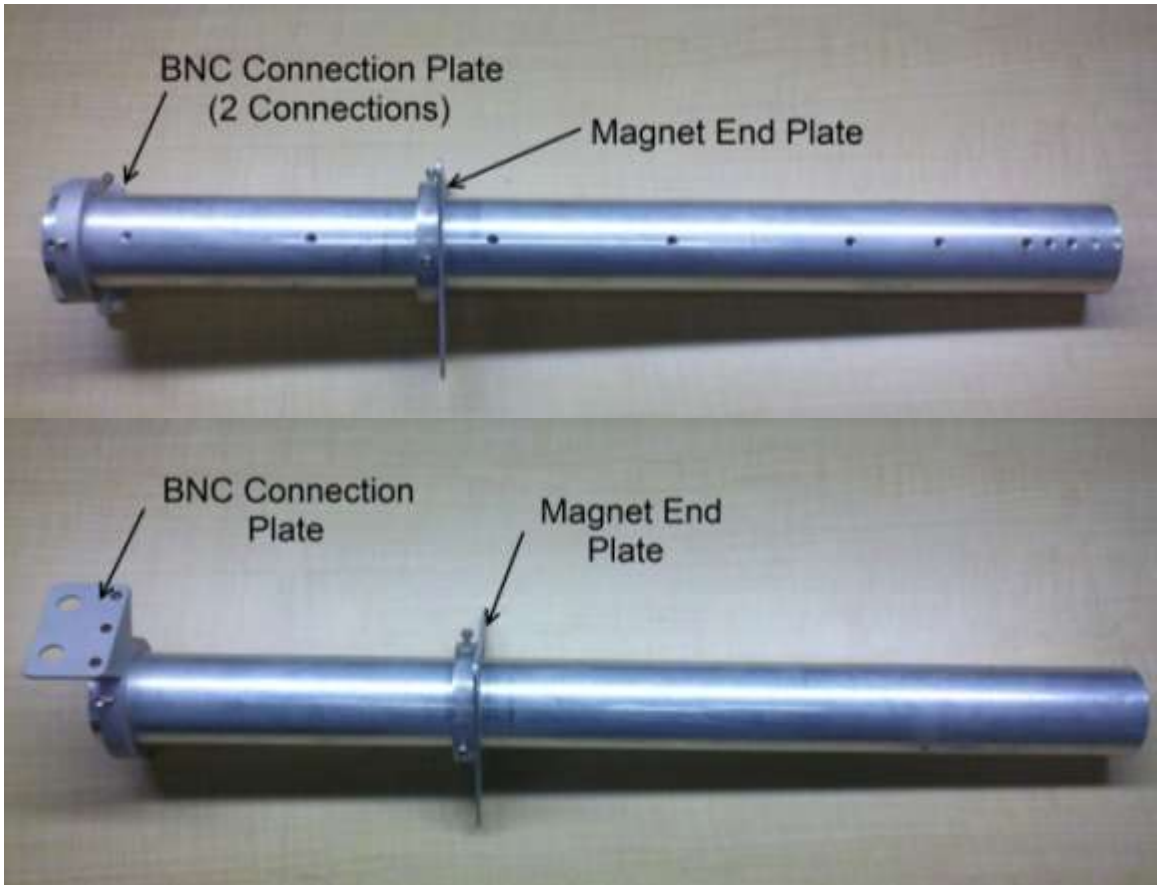

Figure 8: The aluminum support casing contains the BNC connection plate and the magnet end plate. All inside supports are attached by screws on one side of the casing.

Inside the metal casing, the secondary structure consists of plastic tubing with a 1.25" outer diameter, procured from McMaster-Carr. The tube stretches the entire length

of the aluminum casing and extends beyond the top. Aside from general support, the tube also serves as the primary animal bed during imaging. A stationary band saw was used to shape the bed, cutting the tubing longways for the top 5.4 inches. The band saw was also used to make notches at the end of the bed which connect the bed to the facepiece.

Figure 9: The internal support tube contains the internal animal bed at one end.

A number of rings were fabricated from Plexiglas to friction-fit the 1.25" tubing. Three rings were cut form ¼" Plexiglas and one was cut from ½" Plexiglas, each with an internal diameter of 1.25". All rings were cut using a laser cutter.

The laser cutter is designed to read primarily *.CDL files. To simplify the design process, a system was developed which allowed the use of SolidWorks part files in sequence with the laser cutter. Because SolidWorks is more intuitive and feature-rich

than the standard laser cutter design software, the conversion system permitted more exact definition of drawings and parts.

After drawing each piece in 2 dimensions as a *.SLDPRT file, the files were resaved as a *.DXF file. During this step, the face on which the 2D part was drawn was selected. As a *.DXF file, the part could be imported as a 2 dimensional drawing by the laser cutter software.

Three types of holes were incorporated into the rings. Four 6-32 size clearance holes were cut to permit the addition of 24" threaded rods which could serve to align the rings and provide additional structural support. While these holes remained in the final design, the threaded rods were not necessary due to the friction fit of the rings on the 1.25" tubing. Three ¼" holes were incorporated to hold the three lines of tubing (2 lines for heating and 1 line for oxygen). Finally, 2 small holes were added for semirigid wire which connects each coil to the BNC connection ports at the base of the casing.

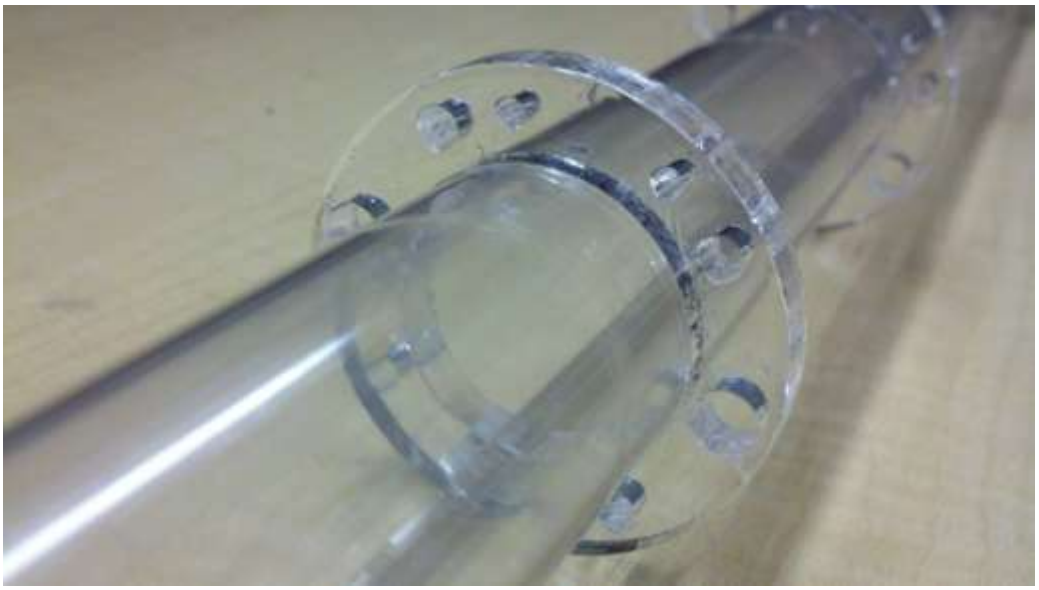

Figure 10: All plastic rings were cut with a laser and friction fit the internal support tube.

Heating

A number of ideas were proposed for body heating during scanning procedures. For humans, heating pads have been designed specifically to keep patients warm during operations. One common design involved an inflatable pad which is connected to two narrow tubes. Hot or warm water is pumped through one arm of the pad and cooled water is removed by the other. This sort of design is desirable for MRI scanning procedures due to the lack of metal or conductive parts. Electric heaters close to the animal's body are potentially dangerous and may cause inhomogeneities in the magnetic field.

A small water-based heating pad was obtained to keep the animal warm, however, it proved to be too big to fit comfortably in the animal bed.

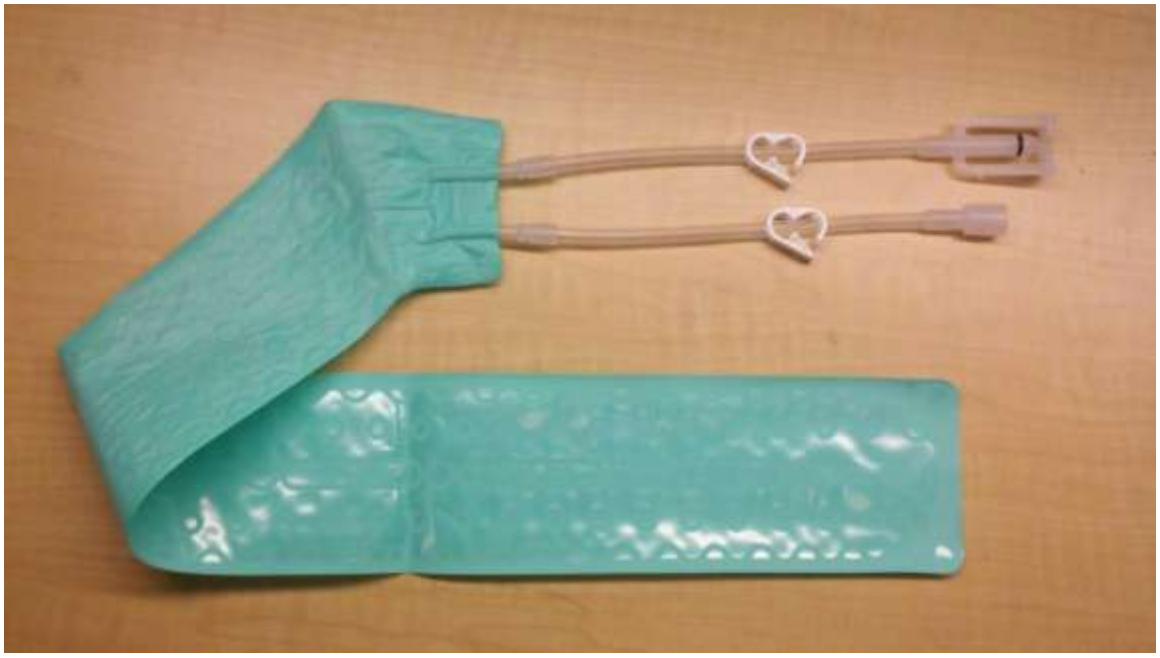

Figure 11: This type of heating pad was considered for the design but did not fit correctly.

A second design approach involved running hot water through ¼” free-standing silicone tubing. By wrapping the tubing around the 1.25” animal bed, enough heat could be transferred to the animal to keep it warm. A moderately sized pump and water heater circulates the water, maintaining the desired temperature as necessary.

Figure 12: Pump used to run water through the heating tube.

Contrary to the previous coil design, an outer bed was attached over the extended section of 1.25” tubing animal bed. The tubing for the outer bed has a 2” outer diameter and 1.75” internal diameter and was procured from McMasters-Carr. The primary purpose of the outer bed is to hold the silicone heating tube encircling the internal bed. The outer tube also serves as increased structural support and protection for the extended section of the RF coil apparatus.

The outer bed was cut using the laser cutter and a stationary band saw. The longitudinal cuts were made by modifying the laser cutter to cut cylindrical objects. Two U-shaped pieces of Plexiglas were cut with a flat bottom edge. By placing each piece upright in the laser bed, the 2” tube could be held still. A strip of plastic was set inside the tube to prevent the laser from cutting through the bottom side. After both cuts were

made, a band saw was used to make the cross sectional cuts, completing the outer bed. One side of the bed was left circumferentially intact for several inches to allow the tube to be connected to the aluminum casing. Holes were made using a drill press for attachments as necessary.

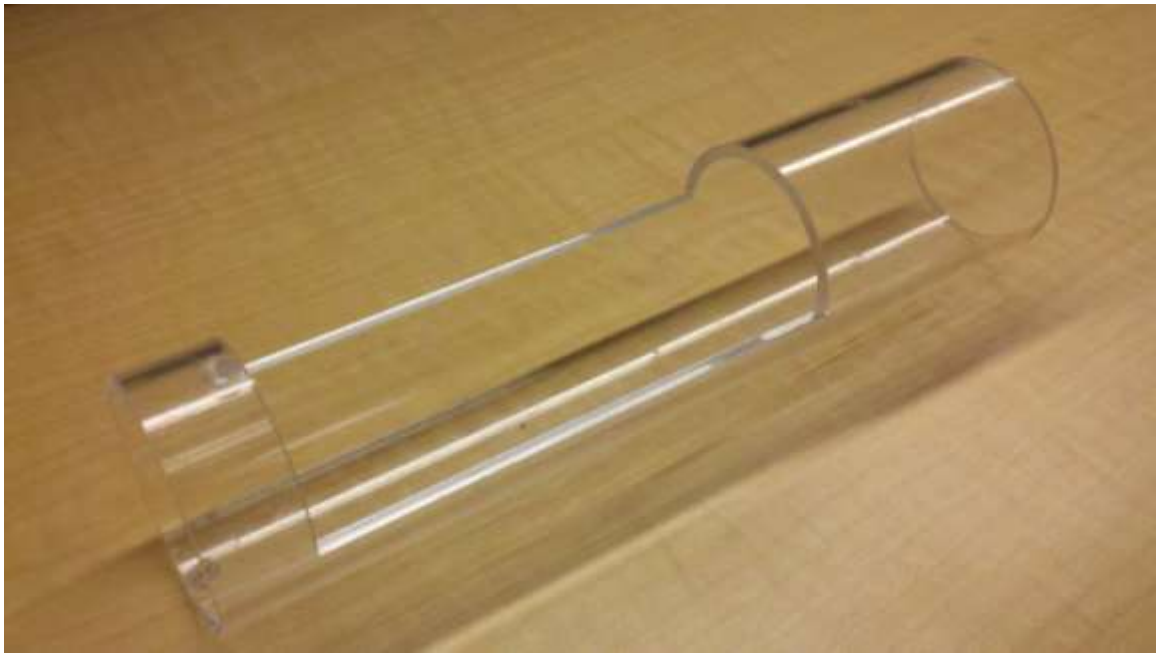

Figure 13: The large bed is 2" in diameter and fits over the internal bed.

The circumferential gap between the internal and outer beds is exactly ¼", allowing the tubing to remain fairly tight in place. ¼" silicone tubing was chosen for its strength and impressive flexibility. Most other types of tubing were prone to kinking, while the silicone remained structurally sound even at relatively tight curvatures. To prevent high signal interference from the water, the tubing could not be placed near the receiving eye resonator. Therefore, a looping configuration was designed which would allow the tubing to surround the bottom and both sides of the internal bed. When filled with hot water, the loops diffuse heat through the internal bed to keep the animal body temperature relatively constant.

Each of the machined Plexiglas rings has two holes to accommodate the ends of the silicone tubing. After exiting the bottom of the aluminum casing, the tubes were left enough length to make connections to extensions leading to the heating pump. The heating pump is both metal and electric and therefore must be kept outside the 5 gauss limit line. Long tube extensions were required to ensure the pump was safe from the magnetic field.

Animal Stabilization

One of the issues identified with the previous design was the tendency of the animal to move significantly due to respiration. To address this concern, several approaches were taken. The primary objective of stabilization is to keep the head of the animal still to limit motion artifacts in the image of the eye. A small plastic bar, termed the "bite bar," was added to the top of the coil which could be adjusted longitudinally. A small hole was cut in one end in which the two front teeth of the animal fit nicely. After setting the animal's teeth in the hole, the position of the head could be adjusted in small increments simply by moving the bar forwards or backwards. In no way did the movement cause any harm to the animal.

Figure 14: The bite bar is made of plastic and has a small hole in one end to fit the animal's front teeth.

While the bite bar was included in previous designs, a new base was necessary to hold the bar. The facepiece which would hold the bar was a critical aspect of the overall design. The apparatus would be responsible for holding the bite bar, the eye resonator, and the air tube. All designs involved attaching a round disk to the end of the large diameter tube to create a cap. By drilling a hole through the cap at approximately 1 inch from the base of the 2” bed (1.75” inside diameter), the bite bar would be at just the right height for an average sized mouse to comfortably attach its teeth. A tapped hole was added to the top of the facepiece to allow a locking screw to be inserted to hold the bite bar in place.

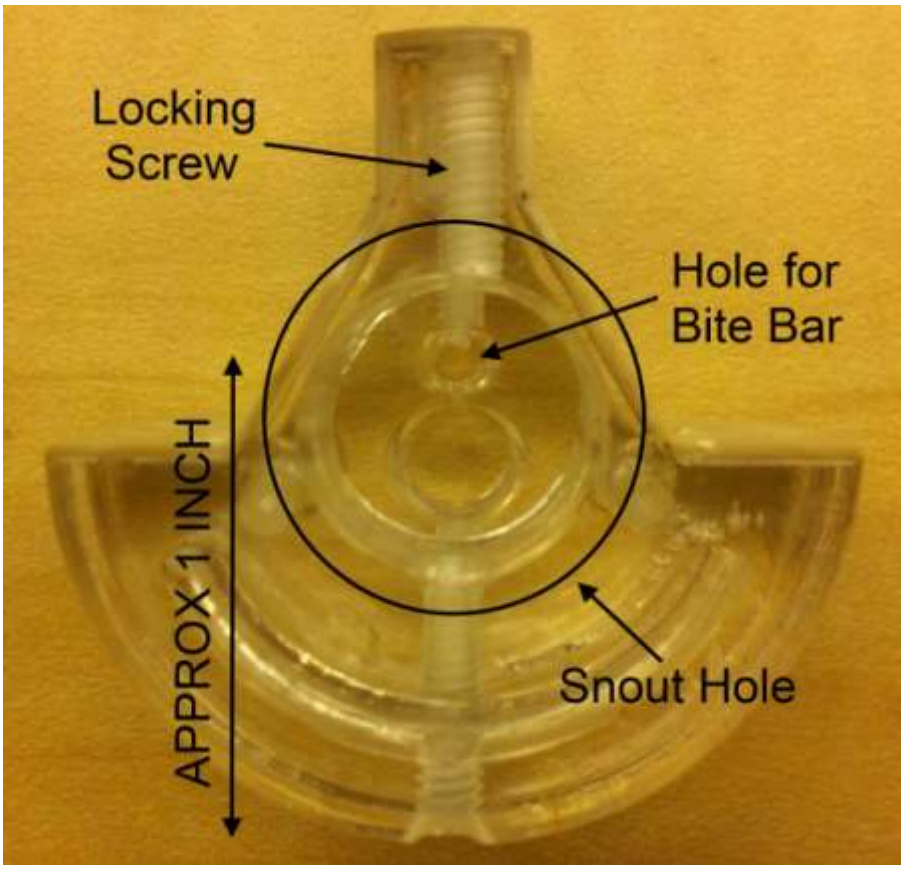

Figure 15: The bite bar is approximately 1" from the base of the facepiece. A screw is used to hold it in place.

A second facepiece similar to the first was created and attached to the first to form a large hole for the snout of the animal. By inserting the bite bar into the small hole and pulling forward, the head of the animal could be drawn forward so its forehead rests against the edge of the hole.

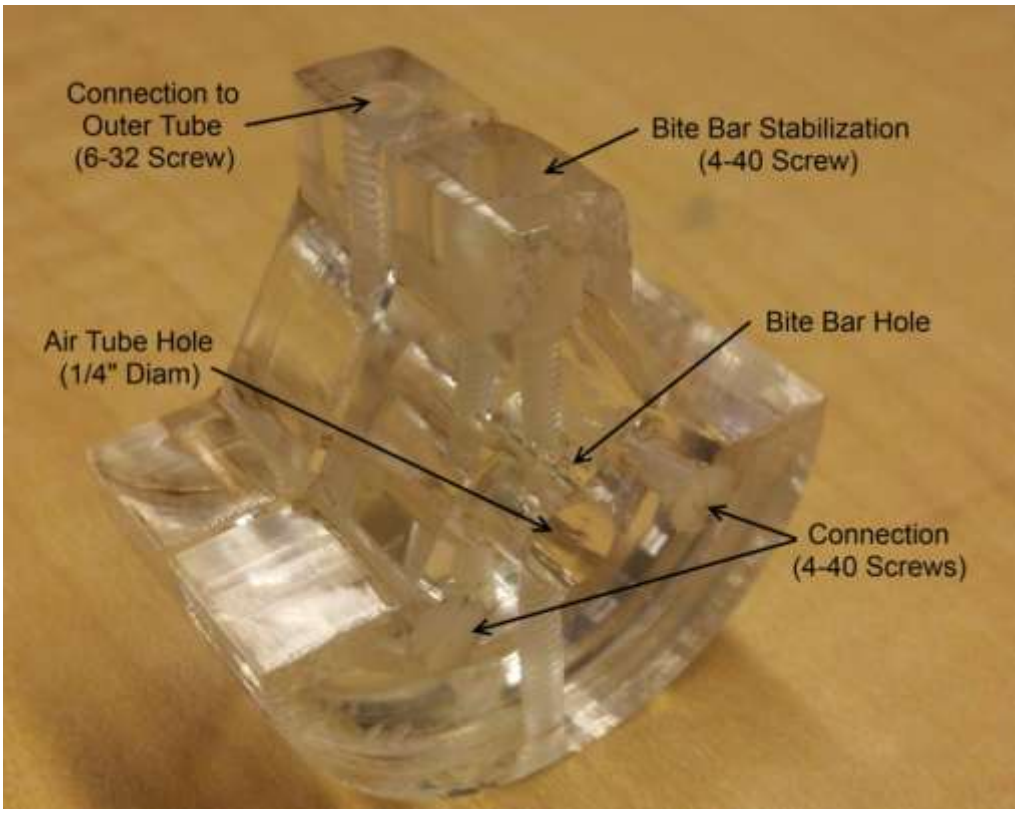

Figure 16: The facepiece consists of two ½" parts which are attaches together by connection screws. All screw identifications are labeled.

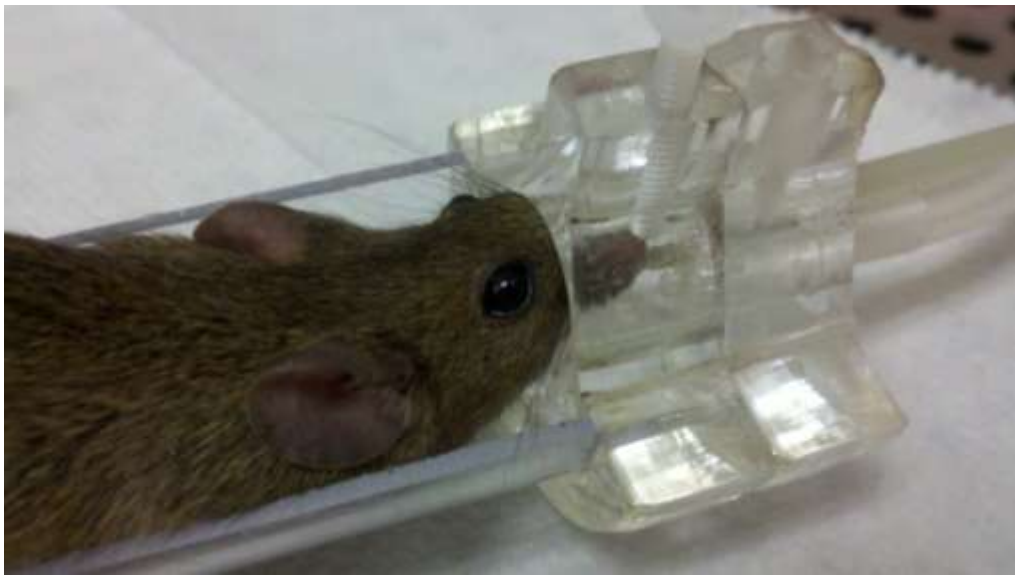

Figure 17: The facepiece holds the snout rigidly to prevent any movement.

In addition to the facepiece and bite bar, medical tape is used for all scans. Unlike the previous design, the animal bed is deep enough for tape to be applied flush to the top of the bed as shown below. With one piece of medical tape applied across the shoulders and a second over the thighs, the animal is held very steady. The head is isolated so that any motion from the rest of the body does not affect the position of the imaging eye.

Figure 18: The animal is stabilized primarily by the bite bar (top) and the facepiece which holds the snout in position. Medical tape is used to isolate the head from all other body movements.

Anesthesia and Oxygen

Throughout the image acquisition, it is necessary to maintain consistent levels of isoflorane gas anesthesia and oxygen. To do so, a tube connection must be made to the top of the coil where the animal's head will be. Each of the machined Plexiglas rings contains a ¼" hole which can accommodate an extra length of silicone tubing similar to that used for the heating unit. The tube extends up through the body of the coil and past the facepiece. The tubing connects to a ¼" hole in the center of the facepiece where it is held in place. On the inside of the facepiece, the tubing hole ejects gas and oxygen directly in front of the animal's snout.

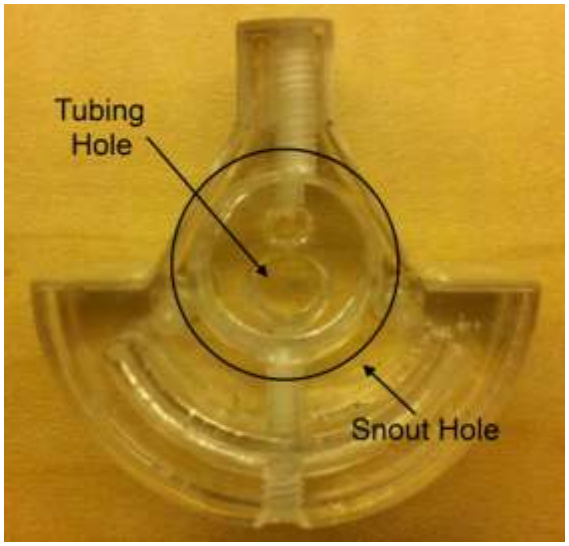

Figure 19: The snout hole of the facepiece encompasses the entrance hole for air tubing to ensure that all oxygen and gas is supplied directly to the animal's mouth and nose.

Eye Radiofrequency Resonator

Originally, several designs were considered for the location of the eye surface resonator. In the original design, the resonator protrudes from the left side of the mouse

and is positioned over the left eye. For the new design, additional freedom of movement was desirable to account for different sized animals. Effort was also made to allow either eye to be scanned rather than limit the resonator to one eye.

As mentioned earlier, the eye resonator was planned to be set on the facepiece in order to remain close to the eye. The first design involved a central hexagon with three slots at different distances from the edges. The resonator would be able to fit through the slots and rest just over the eye. Because the hexagon could be rotated, the resonator could be shifted outwards away from the eye by using a slot closer to the outer edge. Additionally, the hexagon easily allows both eyes to be reached by the resonator with only minor adjustments. Three holes in the center accommodate the bite bar in any configuration.

Figure 20: The hexagon design was considered as a possible way to adjust the eye resonator.

Unfortunately, the slots did not provide sufficient space for the resonator to be easily adjusted laterally (further into or out of the slot). The capacitors required for

matching and tuning were at least twice as thick as the slots, preventing them from sitting sufficiently close to the loop of the resonator. While the design could have been adjusted, it was decided that a simpler design would be more effective.

For the final design, an open triangular pattern was used (see Figure 15 and Figure 16). The new pattern allowed more effective inward and outward movement of the resonator and capacitors to adjust for larger or smaller animals. In addition, the new pattern improved the location of the air tube and bite bar to make the facepiece overall more effective. The surface resonator was mounted on a slotted piece of PC board, selected for its copper surface. A screw on each of the 60 degree surfaces allowed the PC board to move about its slot. In the pilot design, only a right eye resonator was built, however a second resonator may be attached for the left eye with a simple cable wire connection to switch between the resonators. It may even be possible to remove the right eye resonator and attach it over the left eye, although this was not performed during initial testing.

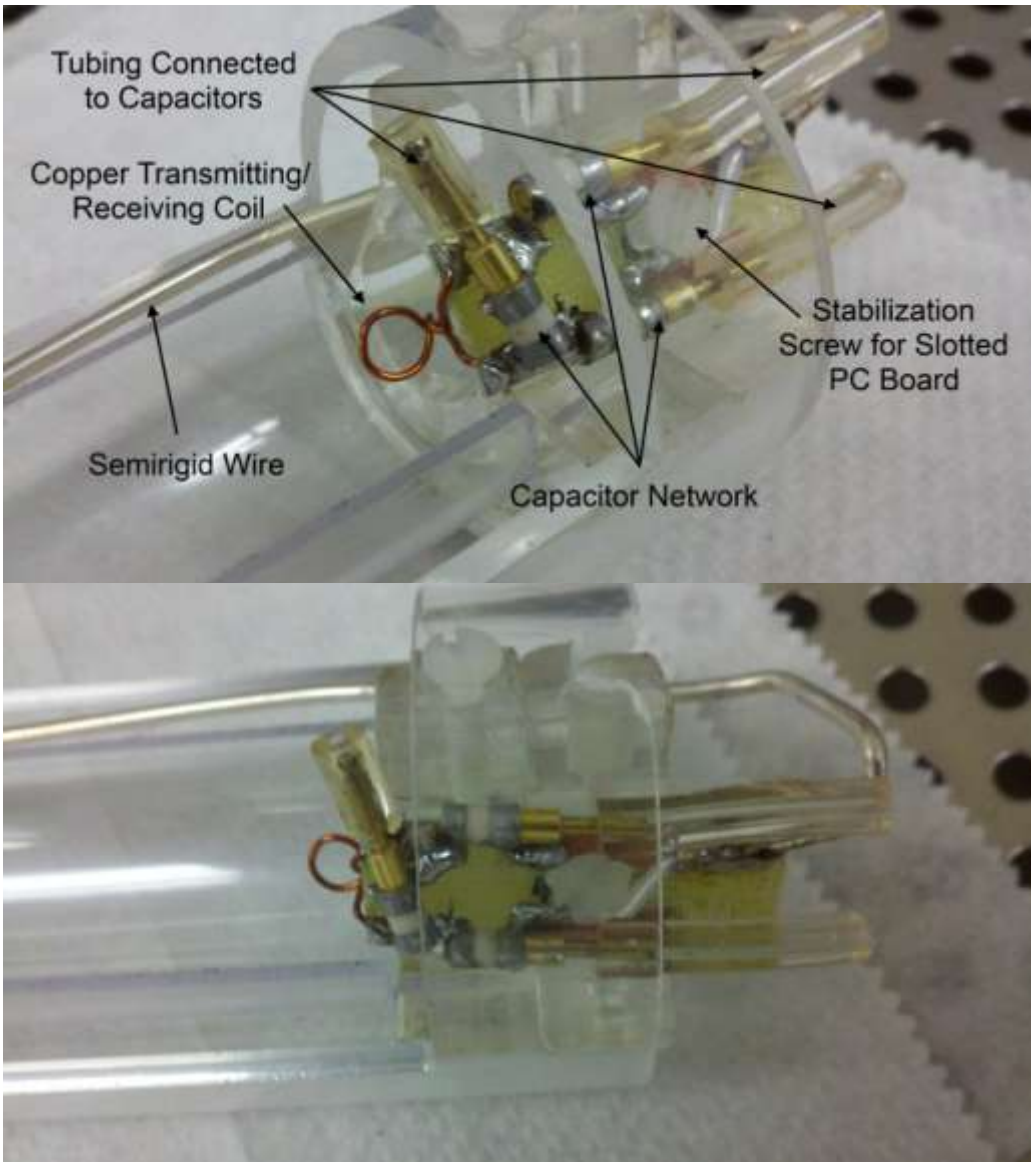

Figure 21: The resonator was placed on PC board and attached to the facepiece using a nonmagnetic screw.

The surface resonator is made out of insulated copper wire with each end soldered to individual strips of copper on the PC board with an internal radius of 0.6 cm. The capacitor network consists of tuning capacitor in parallel to the two matching capacitors in series. The outside casing of a semirigid wire is soldered to one side of the circuit while the inside wire is soldered to the other to complete the circuit. From the PC board,

the semirigid wire is fed through the support rings to the BNC connection on the bottom plate of the aluminum casing. An additional ring was cut out of PC board and connected to the semirigid wire to ground the current.

Due to the small size of the capacitors, short sections of plastic tubing were attached to the screw heads. The capacitor screws may be adjusted by turning the tubing relatively easily. However, when the capacitor reaches its adjustment limit, the tube rotates in place to prevent overturning.

Chapter 4

Methods

Figure 22: Image of 14T Varian Imaging System used to generate the images for analysis, PSU

For all imaging, a vertical wide bore 600 MHz Varian MRI System was used in combination with a custom built RF resonator designed to hold C57BL/6 mice for the duration of the imaging sequence.

The mice subjects are housed in an animal facility located on the same floor as the magnets in the High Field MRI Facility and are managed according to all IACUC protocols. During the imaging process, a respiratory pressure pad was used to monitor the respiratory rate of the animal. A combination of isoflorane gas (1.5-2%) and oxygen (30%) was used to keep the animal unconscious during image scans to prevent movement and discomfort. Additionally, eye lubricant was placed on the eyes to prevent them from drying out during longer scans.

Chapter 5

Results

Surface Coil Gradient Echo Imaging

Figure 23 contains some of the images collected during a past experiment at the High Field MRI Lab at Penn State using the prior coil design (Neuberger, et al., 2008). The left mouse eye is clearly seen in the center of the image. A large blood vessel is visible to the top and right of several of the slices behind the eye, especially those in the second row of images. The retina and choroid layers are fairly distinguishable in many of the slices. Retinal blood vessels appear as black dots along the retina as the excited blood leaves the image field of view (FOV) and new blood enters in. Unfortunately, only a couple vessels are visible along the retinal layer. For this imaging experiment, the thickness of the retina was observed for wild type and diabetic mice. Luan has suggested that some thinning of the retina is present in subjects with diabetic retinopathy (Luan H, 2006). No statistically significant differences between wild type and diabetic mice were found to support this claim from these images (Neuberger, et al., 2008).

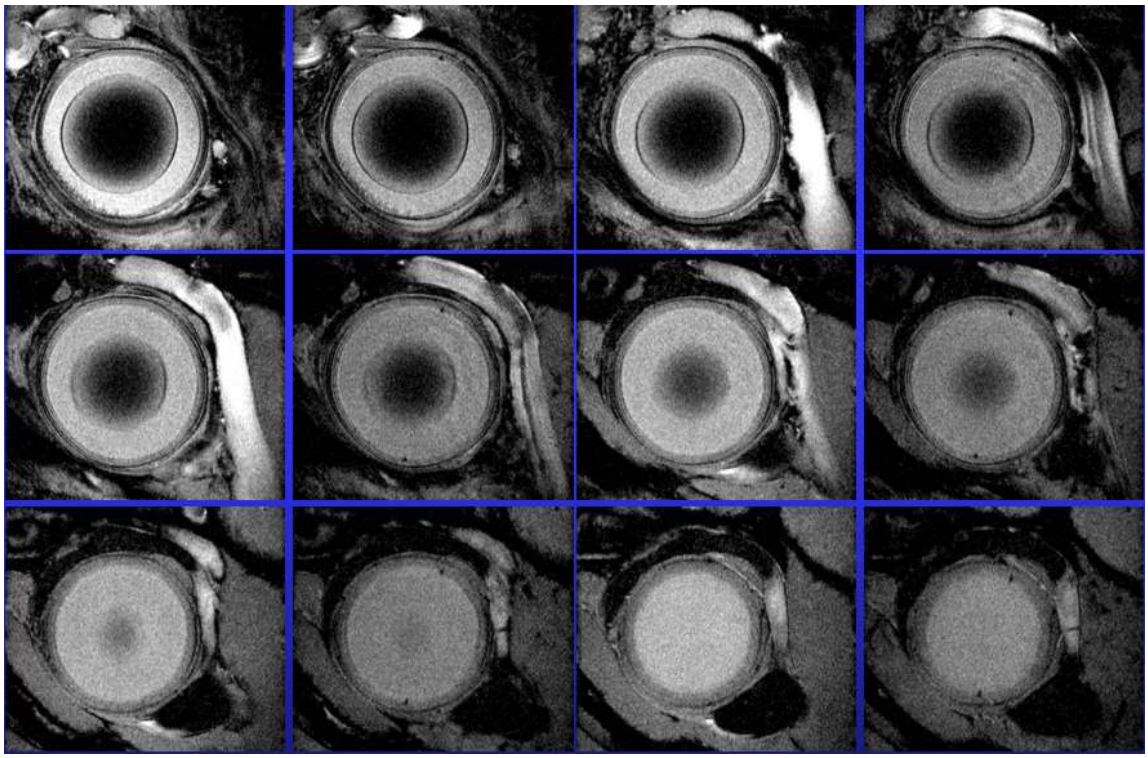

Figure 23: Image from PSU High Field MRI Lab; Gradient echo, TR 200 ms, TE 8.56 ms, matrix size 192 X 264, FOV 6 X 8 mm, 16 averages, Texp 10.6 min, in-plane resolution 30 X 30 micrometers, slice thickness 100 micrometers

To identify a larger number of vessels, higher quality images are necessary. Figure 24 shows a later set of images gathered from a mouse eye using the previous coil. The purpose of this imaging experiment was to reproduce the visual separation between the choroid and retina achieved previously. Despite the fine resolution of 27 μm, the retinal and choroid layers were fairly indistinguishable at most points. With a retinal thickness of approximately 80 μm and a choroid thickness of approximately 42 μm (see Figure 2), this resolution should easily allow layers to be identified. The most likely reason for the lack of contrast between the layers is the presence of motion artifacts (shown with arrows in Figure 24 and Figure 25) due to respiration and circulation.

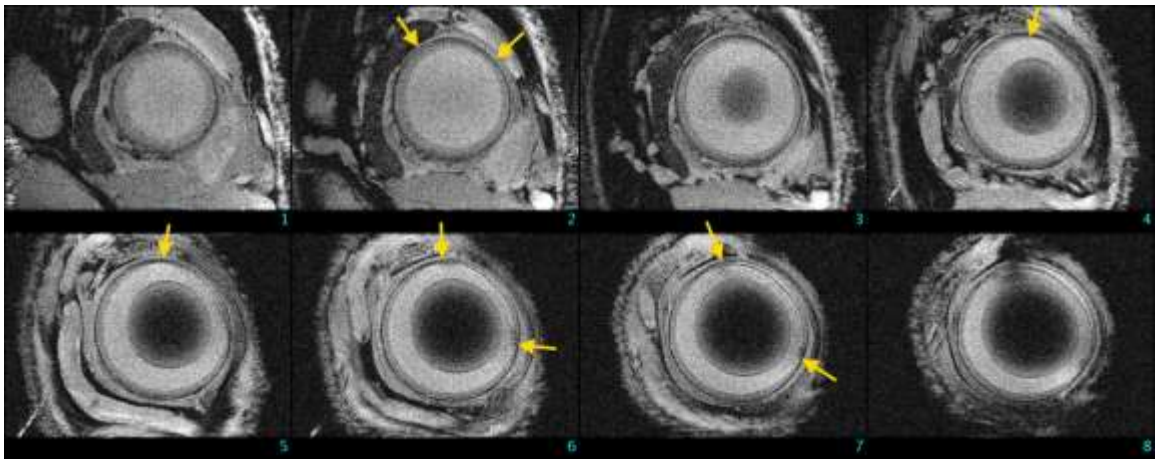

Figure 24: Image of mouse eye; Gradient echo, TR 250 ms, TE 5.79 ms, flip angle 20 degrees, matrix size 186X256, FOV 5X7 mm, 12 averages, resolution 27X27 micrometers, slice thickness 100 micrometers, zerofilled to 1024X1024

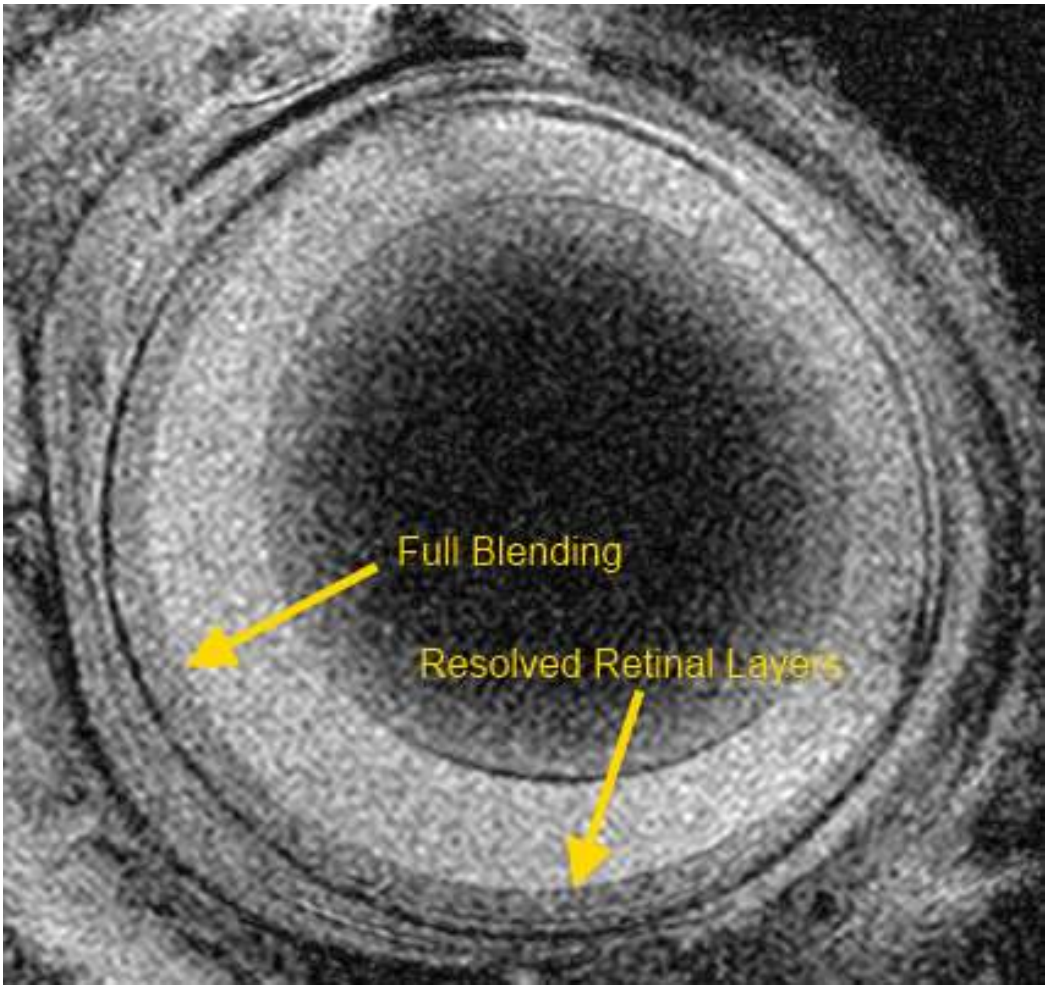

Figure 25: Zoom of Image 7 in Figure 24

The retina and choroid layers are shown as separate layers which become blended into a single layer. If the motion of the eye during the imaging sequence was at least 50-100 μm, the layers would show this sort of blending as the layers become superimposed. This imaging experiment was part of the reason for the design requirement for increased animal stabilization.

The imaging sequence may be altered to account for movement as well. For this image and the image shown in Figure 26, the imaging sequence included 12 averages to increase signal-to-noise ratio (SNR). Rather than performing multiple averages for each image, 12 individual experiments with a single average may be collected. After compiling the images, they may be superimposed using structural features and high signal areas to align the images exactly using MATLAB or another image processing tool. By manually superimposing the images, any small shifts may potentially be corrected. Alternatively, any images which show a large shift from the others may be discarded. This customization is not as easy when collecting multiple averages in the course of a single imaging sequence.

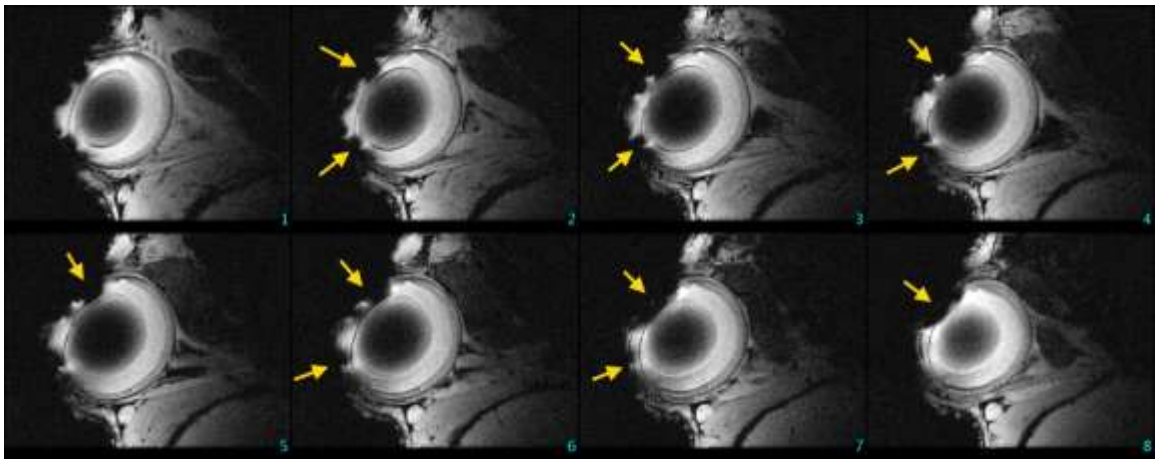

Figure 26: Image of mouse eye; Gradient echo, TR 250 ms, TE 6.95 ms, flip angle 20 degrees, matrix size 186X256, FOV 6X8 mm, 12 averages, resolution 23X23 micrometers, slice thickness 200 micrometers, zerofilled to 1024X1024

A further imaging experiment was performed using the previous coil design to try to distinguish the choroid and retinal layers. Figure 26 contains susceptibility artifacts as shown by the low signal regions on the surface of the eye (yellow arrows on Figure 26). These artifacts resulted from pockets of air becoming trapped between the eye lubricant and the eye. While this artifact was not present on every set of images, care must be taken in future scans to prevent air from becoming trapped near the eye. Figure 26 also shows the same blending representative of potential motion artifacts. In both sets of images, no blood vessels are easily seen along the retina, although the optic nerve is seen exiting the back of the eye in Figure 26. The need for a new radiofrequency coil was determined in large part due to the lack of clear blood vessels in the images collected with the old coil.

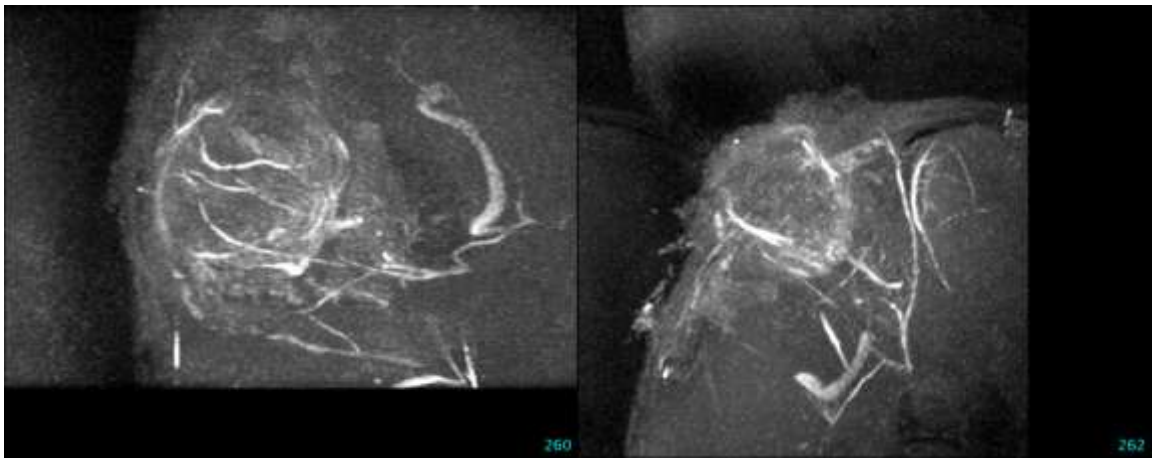

Figure 27: Image of mouse eye; 3D Gradient echo, hard pulse 100 microsec 33 dB, TR 30 ms, TE 2.72 ms, matrix size 128X128X128, FOV 6X9X9 mm, 2 averages, resolution 27X27 micrometers

Figure 27 shows an angiogram of a mouse eye using a 3D gradient echo pulse sequence used to image the blood vessels in and around the eye. A 3D MRI angiogram is similar to other retinopathy detection techniques in its ability to detect new vessels after neovascularization. Time-of-flight MRI was used for these images. This technique involves saturating the entire region during the gradient echo sequence so that only fresh blood entering the vasculature is excited. In the resulting image, only the blood vessels show high signal. Several of the major vessels are evident, outlining the shape of the eye. To detect neovascularization, very small vessels must be visible which are not evident in this image set. In addition, the detection of neovascularization retains the same drawbacks of other detection methods, notably the progression of the disease necessary for diagnosis. One effective use for the 3D angiogram is the identification of large vessels prior to subsequent 2D image sets focusing on perfusion.

New Coil Design

The eye loop of the new coil design did not prove to be stable during initial imaging tests. Inconsistencies are attributed primarily to the shape of the eye loop and the matching and tuning consistency of the capacitor network. Future work will include minor adjustments to both the shape of the loop and the placement of capacitors. In particular, it is desired to keep the capacitors as close as possible to the loop to eliminate excess inductance. In addition, it may be possible to decrease the diameter of the initial loop in order to focus the resolution more precisely on the retina. Overall animal stabilization showed qualitative improvements and simplification over the old design, however, quantitative results could not be obtained from the coil to determine the true effects during scans. The heart resonator could not be completed until the eye resonator is able to successfully generate images at the correct 600 MHz frequency.

Chapter 6

Conclusion

The gradient echo sequences clearly showed many of the structures of the eye including some of the vasculature. However, the detail was not sufficient to begin comparing VEGF-induced vessels to existing vessels in the retina. The obtained resolution was well within the range of the retinal thickness, although motion artifacts limited the image quality. In the future, single-average images may be image aligned in order to offset some of this error.

It was determined that a new coil was needed to achieve the desired resolution and image quality. Preliminary analysis show the coil to be effective in limiting head motion. The eye resonator was completed and its placement was flexible to accommodate different sized subjects. However, the coil was not stable during initial tests and requires further modification before imaging may commence.

Future Studies Using the Custom RF Coil

The construction of this coil is the first major block in a larger investigation of the use of MRI in the diagnosis of diabetic retinopathy (DR). Before experimental imaging can begin, a heart resonator will be constructed which will sit in the internal animal bed directly under the animal's heart. According to Muir, a coil size of approximately 0.8 cm internal diameter is sufficient for arterial labeling (Muir, 2010).

Once a high resolution is obtained using the eye resonator, the specific sequence can be used to increase the signal of the eye vessels. The imaging sequence consists of a

saturation pulse which saturates the endogeneous water in the blood leaving the heart. When the blood reaches the eye, a gradient echo sequence acquires the signal of the eye tissue without the signal from the blood. Afterwards, another gradient echo acquires the signal of both the blood and the eye tissue. By taking the signal difference between the two images, only the signal of the blood will remain. Once the imaging parameters for this sequence are determined, the next phase may begin.

In order to mimic the effects of retinopathy in the animal subjects, vascular endothelial growth factor (VEGF) will be injected approximately one day before scanning. VEGF is known to be effective for imaging purposes for about 72 hours after injection. The injection will take place directly into the eye as necessary. Once inside the eye, the VEGF will begin to promote the growth of new vasculature in the retina. This process mimics the effect diabetes has on the retinal blood vessels. Once the growth process is started, imaging may commence.

After the images of the new vasculature are collected, they may be compared to images taken before the injection. Perfusion rates will be measured in both cases using an appropriate contrast agent. If the technique is successful, decreased levels of perfusion may be observed in animal subjects with induced neovascularization using injected VEGF.

Works Cited

Aiello, L. P. (1995). Vascular Endothelial Growth Factor In Ocular Fluid of Patients with Diabetic Retinopathy and Other Retinal Disorders. *Retina* , 176.

Berkowitz, B. A. (2003). Regulation of the Early Subnormal Retinal Oxygenation Response in Experimental Diabetes by Inducible Nitric Oxide Synthase. *Diabetes* , 173-78.

Bhavsar, A. R. (2011). Diabetic Retinopathy. *Medscape Reference* .

Cheng, H. G. (2006). Structural and Functional MRI Reveals Multiple Retinal Layers. *Proc. Natl. Acad. Sci.* , 17,525-7,530.

Cunha-Vaz, J. G. (1978). Pathophysiology of Diabetic Retinopathy. *British Journal of Ophthalmology* , 351-55.

Laatikainen, L. a. (1976). Fluorescein Angiography and Its Prognostic Significance in Central Retinal Vein Occlusion. *British Journal of Ophthalmology* .

Luan H, R. R. (2006). Retinal thickness and subnormal retinal oxygenation response in experimental diabetic retinopathy. *Invest Ophthalmol Vis Sci* , 47: 320-328.

Muir, E. R. (2010). MRI of Retinal and Choroidal Blood Flow with Laminar Resolution. *WileyOnlineLibrary* .

Neuberger, T., Aussenhofer, S., Kennet, M., Gardner, T., Barber, A., Smith, N., et al. (2008). *Morphological Imaging of the in vivo Mouse Eye: Applications to Diabetic Retinopathy.* Penn State University.

Sicard, K. Q. (2003). Regional Cerebral Blood Flowand BOLD Responses in Conscious and Anesthized Rats Under Basal and Hypercapnic Conditions: Implications for Functional MRI Studies. *Cereb. Blood Flow Metab* , 472-81.

Trick, G. L. (2008). MRI Retinovascular Studies in Humans: Research in Patients with Diabetes. *NMR in Biomedicine* , 1003-012.

Academic Vita **Spring 2012**

Kealan C. Hobelmann

(c) 202-330-1951
kealanhobelmann@gmail.com

Education

Penn State University, Schreyer Honors College, University Park, PA 2008-2012
Bachelor of Science in Nuclear Engineering
Honors in Bioengineering
Thesis: Magnetic Resonance Imaging as a Diagnostic Tool in the Detection of Diabetic Retinopathy in Mice

Work Experience

Bechtel Power Corporation, Frederick, MD 2011
Centralized Analysis Group

Bechtel Power Corporation, Frederick, MD 2010
Mechanical/Nuclear Summer Hire: Nuclear Operating Plant Services Project

Honors/Awards

BSA Eagle Scout Rank
Penn State Student Leader Scholarship
Leonhard Engineering Honors Program
William Leonhard Engineering Scholarship
Carl A. Kroch Oxford Cup Scholarship
Paul Marrow Engineering Scholarship
Schreyer Academic Honors Scholarship
Dean's List 2008-2012 (all semesters)

Activities/Leadership

Beta Theta Pi Fraternity, Alpha Upsilon Chapter 2009-2012
Chapter President, Interfraternity Council Representative, National Convention Delegate, THON Chair

Skull and Bones Senior Honor Society 2012

Campus Crusade for Christ 2008-2012
Bible Study Leader

Alpha Fire Company, State College, PA: Volunteer Firefighter 2008-2010
PA State Firefighter I Certification, National Proboard Firefighter Certification, First Aid/CPR Certification